Computational fluid dynamic analysis following recurrence of cerebral aneurysm after coil embolization

Keiko Irie, Hitomi Anzai[I], Masahiko Kojima[2], Naomi Honjo[3], Makoto Ohta[I], Yuichi Hirose, Makoto Negoro

Department of Neurosurgery, Fujita Health University, [1]Department of Fluid Science, Tohoku University, [2]Department of Micro-Nano System Engineering, Nagoya University, [3]Department of Neuro-Radiology, Osaka Neurosurgery Hospital, Toyoake city Aichi 470-1192, Japan

ABSTRACT

Hemodynamic factors are thought to play important role in the initiation, growth, and rupture of cerebral aneurysms. However, hemodynamic features in the residual neck of incompletely occluded aneurysms and their influences on recanalization are rarely reported. This study characterized the hemodynamics of incompletely occluded aneurysms that had been confirmed to undergo recanalization during long-term follow-up using computational fluid dynamic analysis. A ruptured left basilar-SCA aneurysm was incompletely occluded and showed recanalization during 11 years follow-up period. We retrospectively characterized on three-dimensional MR angiography. After subtotal occlusion, the flow pattern, wall shear stress (WSS), and velocity at the remnant neck changed during long-term follow-up period. Specifically, high WSS region and high blood flow velocity were found near the neck. Interestingly, these area of the remnant neck coincided with the location of aneurysm recanalization. High WSS and blood flow velocity were consistently observed near the remnant neck of incompletely occluded aneurysm, prone to future recanalization. It will suggest that hemodynamic factors may play important roles in aneurismal recurrence after endovascular treatment.

Key words: Cerebral aneurysm, endovascular treatment, hemodynamics recanalization, wall shear stress

Introduction

Cerebral aneurysms are treated by means of either endovascular coiling or surgical clipping. Despite their widespread use, these therapeutic modalities are not always successful in eliminating the risk of subsequent aneurysm rupture and subarachnoid hemorrhage (SAH). Regarding the coiling technique, one of the primary failure mechanisms leading to aneurysm regrowth, recanalization, and rebleeding is coil compaction.[1,2] The aneurysms with remnant necks after endovascular occlusion are prone to recanalization, whereas the underlying mechanisms of this phenomenon are not totally clear.[3,4] We

have a primary interest in the hemodynamic influences in recanalization of partially occluded aneurysms.

Yet, even in the best cases, the coiling material accounts for less than 50% of the total treated aneurysm volume.[5,6] Consequently, coil compaction can occur and is especially problematic for giant aneurysms, large aneurysms containing thrombi, and aneurysms that project along the direction of blood flow in the parent artery. In addition, loose packing of coils can lead to coil unraveling and migration into the parent artery and subsequent aneurysm regrowth. Numerous evidences suggest that the intra-aneurysmal hemodynamic patterns may have a profound impact on the development of ceral aneurysms. Using computational fluid dynamics (CFD) analysis, researchers have identified that high-velocity and high-shear stress of the flow impingement may have positive effects on the growth of cerebral aneurysms.[7-9] The aim of the present study was to characterize the hemodynamic changes of the partially embolized aneurysms that were predisposed to recanalization in a long term.

Materials and Methods

Clinical and imaging data

A 58-year-old female patient presented with headache and

Address for correspondence:
Dr. Keiko Irie, 1-98 Dengakugakubo, Kutsukake, Toyoake, Aichi 470-1192, Japan. E-mail: kirie@fujita-hu.ac.jp

SAH in July 2000. Angiography revealed left basilar-SCA small aneurysm [Figure 1a]. This aneurysm was treated via endovascular embolization with coils. Immediately after coil embolization, the aneurysm was completely occluded and the left superior cerebellar artery (SCA) was preserved [Figure 1b]. The patient could not come for follow-up due to her schedule, and we could not follow up at the outpatient clinic. Six years after the initial coil embolization, we noticed a small neck remnant at 3D-MRA. The neck remnant gradually enlarged and cerebral angiography showed recurrence of the aneurysm [Figure 2]. Then, coil embolization was carried out again in March 2007. Immediately after the coil embolization showed disappearance of the aneurysm and preservation of SCA, but a remnant was observed at the SCA origin [Figure 2b]. The follow-up using 3D-MRA revealed re-enlargement of the remnant neck to recanalize the aneurysm to drastically grow further [Figure 3], and it ruptured in May 2011.

Hemodynamic modeling

A patient-specific CFD model of the aneurysm was constructed from the 3D-MRA image using previously developed methods.[10] The image was filtered, and segmentation was performed with a seeded region growing algorithm to reconstruct the topography of the vascular network followed by an isosurface deformable model to adjust the geometry to the vessel boundaries.[11] The vascular model was then smoothed with a nonshrinking algorithm, and the vessels were truncated perpendicularly to their axes. A volumetric grid composed of tetrahedral elements was generated by an advanced front method with a resolution of 0.15 mm, including three layers prism-layered mesh with a resolution of 0.01 mm, resulting in approximately a 3.2 million-element mesh.

After meshing, we used ICEM CFD software 13.0 (ANSYS Inc., Berkeley, CA, USA) to generate the configuration files that specified the settings of blood properties, boundary conditions, and the time step for fluid field computation. Concerning the calculation scheme, three-dimensional segregated solver and second-order implicit formulation
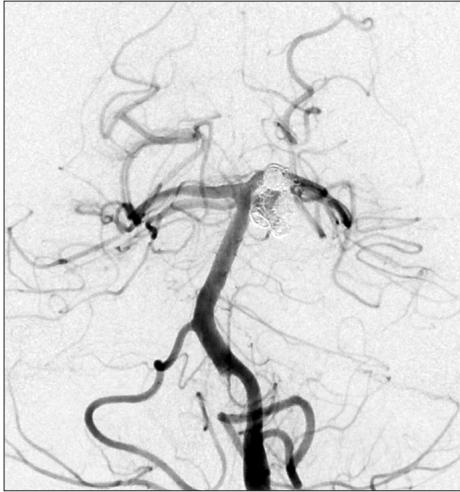

Figure 1: (a) Cerebral angiography revealed left basilar-SCA small aneurysm; (b) Immediately after coil embolization, the aneurysm was completely occluded

Figure 2: (a) Seven years after the initial coil embolization, cerebral angiography showed recurrence of the aneurysm; (b) Immediately after the second coil embolization showed disappearance of the aneurysm, but a neck remnant was observed

in time were selected. Blood flow was considered as an incompressible non-Newtonian fluid and modeled by the unsteady Navier-Stokes equations in 3D. The vessel walls were assumed rigid, and no-slip boundary conditions were applied at the walls. The average Reynolds number was within the range of normal blood flow in the human cerebral arteries, indicating a laminar flow condition. The density and dynamic viscosity of blood were specified as 1050 kg/m^3 and 0.0035 mPas, respectively. The pressure-velocity coupling method was SIMPLE, and the pressure term was solved by the PRESTO

Figure 3: Four years after the second coil embolization, cerebral angiography revealed re-enlargement of the remnant neck to recanalize the aneurysm to drastically grow further

method. Momentum term of Navier-Stokes equation was discretized with the second-order upwind difference scheme and solved by algebraic multigrid (AMG).
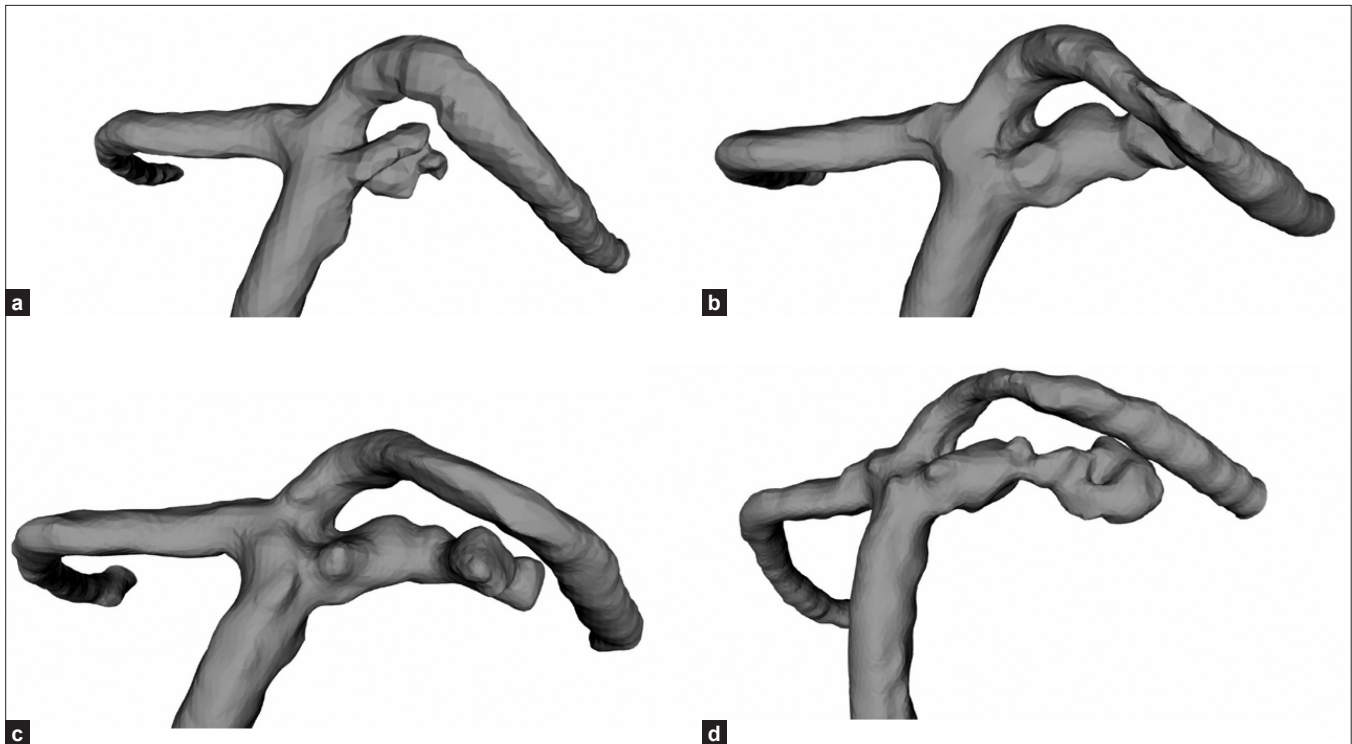
Results

Aneurysm geometries

The 3D aneurysm geometry was prepared based on the 4-year follow-up 3D-MRA DICOM data of the patient. A neck remnant was observed in April 2008; i.e. 1 year after second coil embolization [Figure 4a]. The subsequent follow-up revealed that the neck remnant kept growing with skewed morphology, and the third coil embolization was carried out as it ruptured in May 2011 [Figure 4b-d].
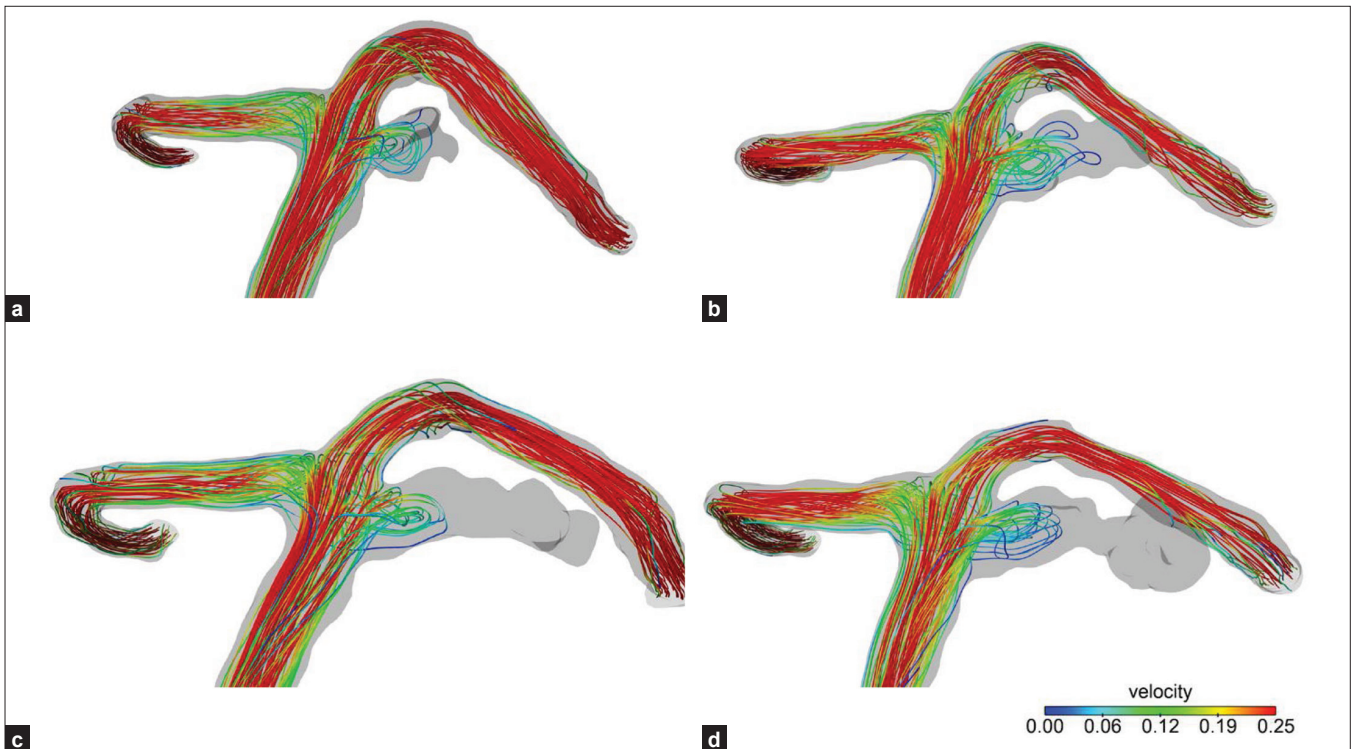
Stream line

After the second coil embolization, blood flow entered the remnant neck and formed a small vortex [Figure 5a]. Subsequent follow-up revealed regrowth of the neck remnant. The blood infiltration (spiral vortex blood flow) was observed only at the neck remnant region while the blood inflow was not observed at the enlarged aneurysm dome [Figure 5b-d]. Vector analysis of the flow velocity revealed that the flow rate at the aneurysm neck was consistently faster than the other aneurysm regions during the follow-up period, and showed the presence of impingement [Figure 6a-d].

### Wall shear stress and pressure

The high-flow regions of the remnant neck matched with the high-WSS regions (impingement regions), and the WSS

Figure 4: The 3D aneurysm geometry was prepared based on the 3D-MRA DICOM data of the patient (a) One year after second coil embolization; April 2007; (b-d) The neck remnant kept growing with skewed morphology, aneurysm ruptured in May 2011

Figure 5: (a) After the second coil embolization, blood flow entered the remnant neck and formed a small vortex; (b, c, d) Spiral vortex blood flow was observed only at the neck remnant region while the blood inflow was not observed at the enlarged aneurysm dome
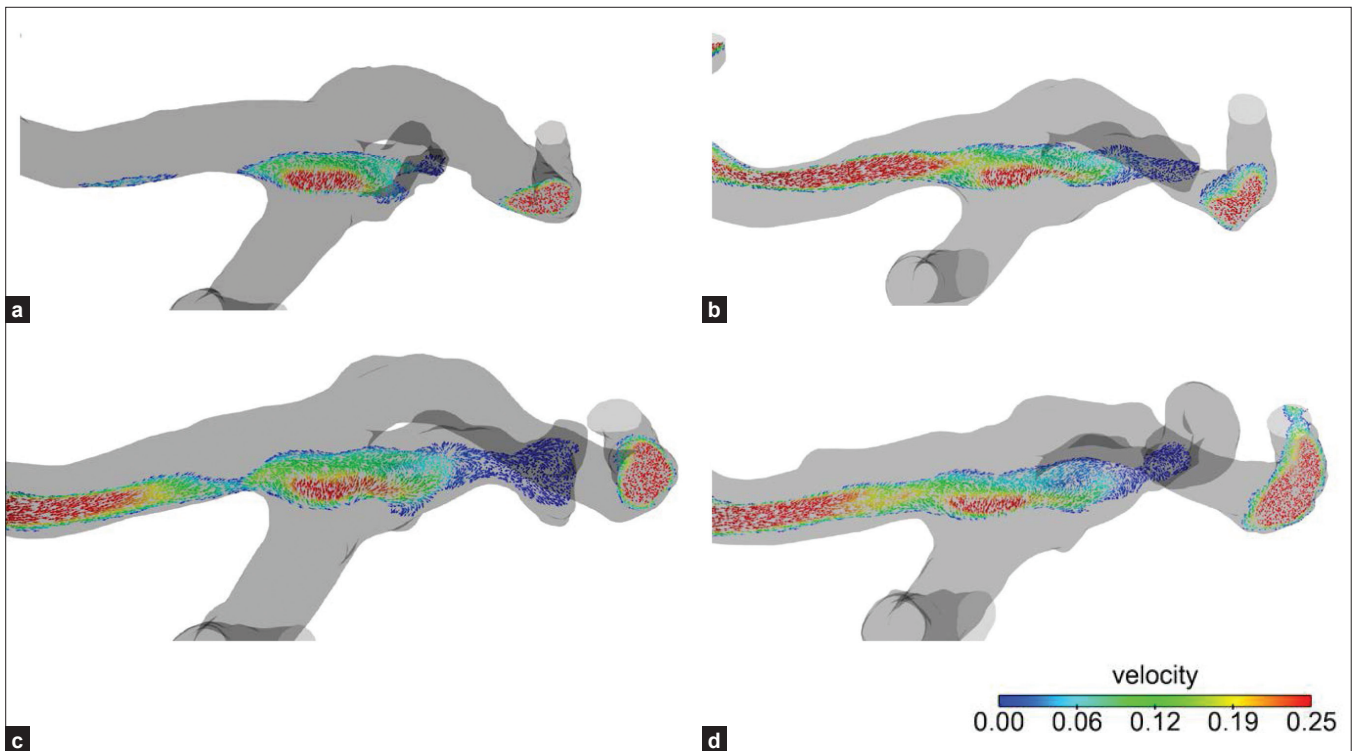

Figure 6: (a-d) Vector analysis of the flow velocity revealed that the flow rate at the aneurysm neck was consistently faster than the other aneurysm regions during the follow-up period, and showed the presence of impingement

gradually decreased at aneurysm dome [Figure 7a-d]. The aneurysm wall pressure tended to be higher at the enlarged aneurysm than at the neck [Figure 8a-d].

Discussion

The long-term follow-up after treatment of cerebral aneurysms
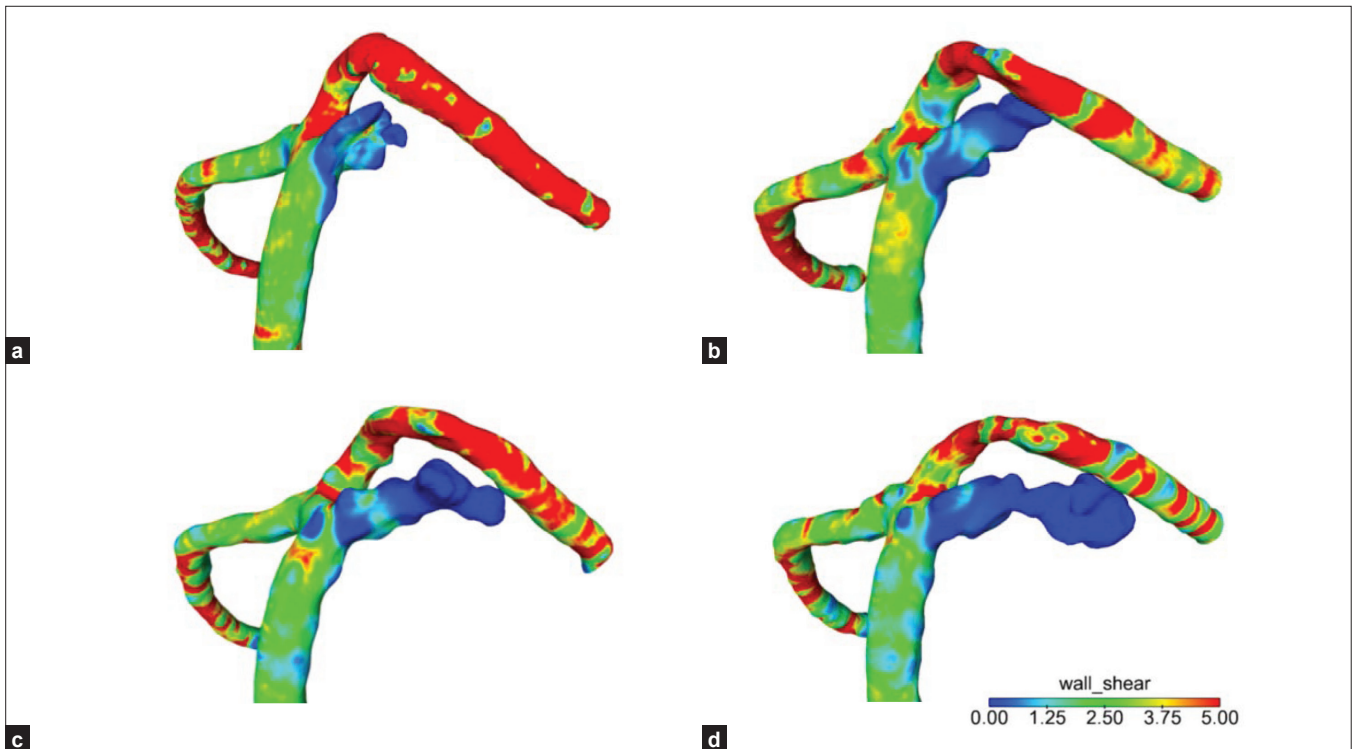
Figure 7: (a-d) The high-flow regions of the neck remnant matched with the high-WSS regions (impingement regions), and the WSS gradually decreased at aneurysm dome
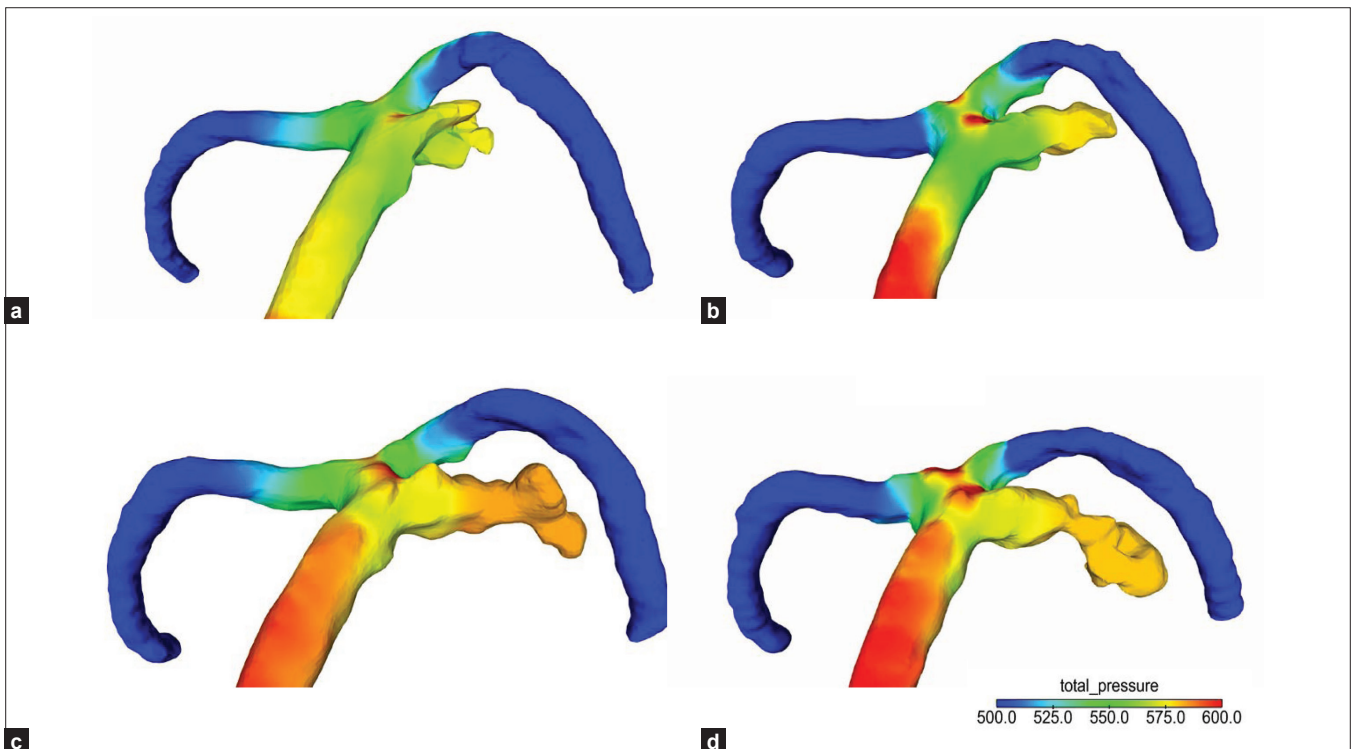
Figure 8: (a-d) The aneurysm wall pressure tended to be higher at the enlarged aneurysm than at the neck

with detachable coils was reported previously. Raymond *et al.*[12] reported the results of 31 aneurysms at the basilar bifurcation. Of the 29 surviving patients, 27 underwent 6-month follow-up angiography, and 12 underwent another follow-up angiographic examination 1 year later. Recurrence or re-growth of the remnant was seen in 7 patients (24%). Cognard *et al.*[1] reported a recurrence rate of 14% in 148 initially totally occluded aneurysms. Remnant regrowth occurred in 6 of 18 subtotally

occluded aneurysms. It is possible that incomplete obliteration modifies the intra-aneurysmal hemodynamic forces and thus may promote the growth and even rupture of some aneurysms.

Angiographically demonstrated complete obliteration of an aneurysm sac after endovascular coil embolization does not mean that the aneurysm sac is completely filled with coils. Computer-assisted analysis of the aneurysm volume and the introduced coil mass revealed that the coil mass did not exceed 30% of the aneurysm sac volume despite complete packing on angiography.[4] Recanalization of the intracranial aneurysms treated with detachable coils depends on various factors including the aneurysm size, neck width, aneurysm location, history of rupture, and immediate post-embolization angiographic results.[1,12,13] Previous studies have shown that recanalization was more common in large and wide-neck aneurysms.[14]

The bifurcation or termination aneurysms reportedly show higher recanalization rate than those of other locations, suggesting that the aneurysm location and hemodynamic stress might be closely related to the risk of recanalization. It is generally considered that the arterial flow stress induces more frequent recanalization.[15]

Cerebral aneurysms are preferentially located at the outer curvatures, bifurcations, or branching points of the brain vessels. As shown by CFD modeling, these vascular segments are affected by complex hemodynamic forces, including impinging flow and alteration of WSS,[15] which may induce pathological remodeling of the vascular structure, transmitted by the endothelial cells.[16,17]

Several studies demonstrated that the residual neck of subtotally embolized aneurysms that underwent subsequent recanalization may be associated with high-flow velocity and WSS.[18,19] An impressive finding is that the high-velocity and WSS region coincided with the location of future aneurysm recanalization. Boet *et al.*[18] stated that the paraclinoid/ophthalmic segment artery aneurysms were more susceptible to recanalization after primary treatment, and they hypothesized that the high-shear stress imposed on the aneurysm in this particular position might contribute to recurrence. Luo *et al.*[19] reported the high-WSS and blood flow velocity were consistently observed near the remnant neck of partially embolized aneurysms prone to future recanalization, suggesting that the hemodynamic factors may have an important role in aneurysmal recurrence after endovascular treatment. Ortega *et al.*[20] performed CFD simulation within a patient-derived basilar aneurysm model. They identified a blood flow impingement adjacent to the remnant neck and found an increase in WSS.

Our results and those of Ortega *et al.*[20] and Luo *et al.*[19] indicated that a localized postembolization high WSS at the remnant neck area might contribute to the development of

recanalization. Elevation of WSS can cause endothelial injury and thus initiates wall remodeling and potential degeneration. Vascular endothelial malfunction and/or abnormal shear stress field can cause overexpression of the endothelium-dependent NO production, leading to a lower, nonphysiological local arterial tone via processes connected to the scarcity and apoptosis of wall-embedded smooth muscle cells and remodeling. This results in disturbance of the equilibrium between the blood-pressure forces and the internal wall stress forces, in favor of the former, and subsequently dilates the arterial wall locally. The resulting abnormal blood shear stress field is the driving factor for further growth of the aneurysmal geometry. This geometrical growth stretches the collagen and elastin fibers of the medial and adventitial layers, leading to internal stress that contributes to the arterial stiffness. Eventually, the biomechanical system equilibrates at a state where the internal wall stresses and the transmural pressure are equal while the local hemodynamics cannot alter the arterial properties any more. At this point, the elastin and the collagen fibers are constantly under a nonphysiologically large mechanical load and eventually undergo remodeling.[21,22] High WSS and fast blood flow may hamper the local blood coagulation process and prevent formation of blood clots inside the aneurysms.[23,24] Furthermore, the pressure caused by high-speed blood flow may lead to coil compaction, especially in aneurysms with a wide neck, which is thought to be a determining factor in recanalization.[3,25]

Our present data revealed that WSS of the enlarged aneurysm dome after recanalization gradually decreased and the aneurysm ruptured. The low WSS within aneurysms was the cause of localized blood-flow stagnation against the wall in the dome. Blood stagnation causes dysfunction of flow-induced NO, which is usually released by mechanical stimulation due to increased shear stress. This dysfunction results in aggregation of the red blood cells, as well as accumulation and adhesion of both platelets and leukocytes along the intimal surface. This process may cause intimal damages, leading to infiltration by white blood cells and fibrin inside the aneurysm wall, all of which have been detected in pathological examinations of aneurysm walls. The inflammation leads to localized degeneration of the aneurysm wall, resulting in a lower pressure threshold at which the physiological tensile forces could be supported. The aneurysm wall progressively thins and finally may cause the tissue to tear. It is considered that some forces applied to the thinned aneurysm wall ultimately cause aneurysm rupture.

Limitation of this study

The case study sample warrants some caution. It is conceivable that this study is not representative of the patient population at large. Moreover, our current study has several limitations common to most CFD analysis, which should be considered when evaluating the results. There are several sources of error that can affect the accuracy of the numeric simulations.

The vascular geometry was approximated from 3D-MRA image data and may have distortions from the process of construction and image optimization. The flow conditions were not patient specific but were derived from measurements on healthy subjects. Several assumptions were made for the CFD calculations, including outflow boundary conditions, rigid walls, and Newtonian properties. The wall biomechanics and perianeurysmal environment were not considered.

Conclusions

High WSS and blood flow velocity were consistently observed near the remnant neck of incompletely occluded aneurysms prone to future recanalization, suggesting that the hemodynamic factors may have an important role in aneurysmal recurrence after endovascular treatment.

References

1. Cognard C, Weil A, Spelle L, Piotin M, Castaings L, Rey A. Long-term angiographic follow-up of 169 intracranial berry aneurysms occluded with detachable coils. Radiology 1999;212:348-56.
2. Kang HS, Han MH, Kwon BJ, Kwon OK, Kim SH. Repeat endovascular treatment in post-embolization recurrent intracranial aneurysms. Neurosurgery 2006;58:60-70.
3. Kai Y, Hamada J, Morioka M, Yano S, Kuratsu J. Evaluation of the stability of small ruptured aneurysms with a small neck after embolization with Guglielmi detachable coils: Correlation between coil packing ratio and coil compaction. Neurosurgery 2005;56:785-92.
4. Choi DS, Kim MC, Lee SK, Willinsky RA, Terbrugge KG. Clinical and angiographic long-term follow-up of completely coiled intracranial aneurysms using endovascular technique. J Neurosurg 2010;112:575-81.
5. Horowitz M, Samson D, Purdy P. Does electro-thrombosis occur immediately after embolization of an aneurysm with Guglielmi detachable coils? AJNR Am J Neuroradiol 1997;18:510-3.
6. Kallmes DF, William AD, Cloft HJ, Lopes MB, Hankins GR, Helm GA. Platinum coil-mediated implantation of growth factor-secreting endovascular tissue grafts: An *in vivo* study. Radiology 1998;207:519-23.
7. Hassan T, Timofeev EV, Saito T, Shimizu H, Ezura M, Tominaga T. Computational replicas: Anatomic reconstructions of cerebral vessels as volume numerical grids at three dimensional angiography. AJNR Am J Neuroradiol 2004;25:1356-65.
8. Tateshima S, Tanishita K, Omura H, Villablanca JP, Vinuela F. Intra-aneurysmal hemodynamics during the growth of an unruptured aneurysm: *In-vitro* study using longitudinal CT angiogram database. AJNR Am J Neuroradiol 2007;28:622-7.
9. Steinman DA, Milner JS, Norley CJ, Lownie SP, Holdsworth DW. Image-based computational simulation of flow dynamics in a giant intracranial aneurysm. AJNR Am J Neuroradiol 2003;24:559-66.
10. Cebral JR, Castro MA, Appanaboyina S, Putman CM, Millan D, Frangi AF. Efficient pipeline for image-based patient-specific analysis of cerebral aneurysm hemodynamics: Technique and sensitivity. IEEE Trans Med Imaging 2005;24:457-67.
11. Yim PJ, Vasbinder GB, Ho VB, Choyke PL. Isosurfaces as deformable models for magnetic resonance angiography. IEEE Trans Med Imaging 2003;22:875-81.
12. Raymond J, Guilbert F, Weill A, Georganos SA, Juravsky L, Lambert A. Long-term angiographic recurrences after selective endovascular treatment of aneurysms with detachable coils. Stroke 2003;34:1398-403.
13. Grunwald IQ, Papanagitou P, Struffert T, Politi M, Krick C, Gui G. Recanalization after endovascular treatment of intracerebral aneurysms. Neuroradiology 2007;49:41-7.
14. Sluzewski M, Brilstra EH, van Rooij WJ, Wijnalda CA, Tulleken CA, Rinkel GL. Bilateral vertebral artery balloon occlusion for giant vertebrobasilar aneurysms. Neuroradiology 2001;43:336-41.
15. Alnaes MS, Isaksen J, Mardal KA, Romner B, Morgan MK, Ingebrigtsen T. Computation of hemodynamics in the circle of Willis. Stroke 2007;38:2500-5.
16. Schimer CM, Malek AM. Wall shear stress gradient analysis within an idealized stenosis using non-Newtonian flow. Neurosurgery 2007;61:853-63.
17. Malek AM, Alper SL, Izumo S. Hemodynamic shear stress and its role in atherosclerosis. JAMA 1999;282:2035-42.
18. Boet R, Wong GK, Poon WS, Lam JM, Yu SC. Aneurysm recurrence after treatment of paraclinoid/ophthalmic segment aneurysm treatment modality assessment. Acta Neurochir (Wien) 2005;147:611-6, discussion 616.
19. Luo B, Yang X, Wang S, Haiyun Li, Chen J, Yu H. High shear stress and flow velocity in partially occluded aneurysms prone to recanalization. Stroke 2011;42:745-53.
20. Ortega J, Hartman J, Rodriguez J, Maitland D. Post-treatment hemodynamics of a basilar aneurysm and bifurcation. Ann Biomed Eng 2008;36:1531-46.
21. Chatziprodromou I, Tricoli A, Poulikakous D, Ventikos Y. Haemodynamics and wall remodeling of a growing cerebral aneurysm: A computational model. J Biomech 2007;40:412-26.
22. Meng H, Wang Z, Hoi Y, Gao L, Metaxa E, Swartz DD. Complex hemodynamics at the apex of an arterial bifurcation induced vascular remodeling resembling cerebral aneurysm initiation. Stroke 2007;38:1924-31.
23. Byun HS, Rhee K. CFD modeling of blood flow following coil embolization of aneurysms. Med Eng Phys 2004;26:755-61.
24. Rays VL, Boussel L, Acevedo-Bolton G, Martin AJ, Young WL, Lawton MT. Numerical modeling of the flow in intracranial aneurysms: Prediction of regions prone to thrombus formation. Ann Biomed Eng 2008;36:1793-804.
25. Renowden SA, Benes V, Bradley M, Molyneux AJ. Detachable coil embolization of ruptured intracranial aneurysms: A single center study, a decade experience. Clin Neurol Neurosurg 2009;111:179-88.

"Quick Response Code" link for full text articles

The journal issue has a unique new feature for reaching to the journal's website without typing a single letter. Each article on its first page has a "Quick Response Code". Using any mobile or other hand-held device with camera and GPRS/other internet source, one can reach to the full text of that particular article on the journal's website. Start a QR-code reading software (see list of free applications from http://tinyurl.com/yzlh2tc) and point the camera to the QR-code printed in the journal. It will automatically take you to the HTML full text of that article. One can also use a desktop or laptop with web camera for similar functionality. See http://tinyurl.com/2bw7fn3 or http://tinyurl.com/3ysr3me for the free applications.